



Using Filters to Estimate Regional Lung Deposition with Dry Powder Inhalers

Scott Tavernini^{1,2} • Dino J. Farina³ • Andrew R. Martin^{1,2} • Warren H. Finlay^{1,2}

Received: 5 May 2021 / Accepted: 11 July 2021 / Published online: 31 August 2020

© The Author(s), under exclusive licence to Springer Science+Business Media, LLC, part of Springer Nature 2021

ABSTRACT

Purpose To develop an in vitro method to rapidly evaluate regional lung doses delivered by pharmaceutical inhalers. Currently, cascade impactor measurements are used, but these are resource intensive and require significant post processing of in vitro data to arrive at regional deposition estimates.

Methods We present a specialized filter apparatus that mimics tracheobronchial (TB) deposition of pharmaceutical aerosols emitted by commercially available dry powder inhalers (DPIs). The filter housing includes an electrostatic neutralizer to eliminate artificial electrostatic filtration effects. Regional deposition (tracheobronchial and alveolar) for four DPIs (Onbrez Breezhaler, Flovent Diskus, Pulmicort Turbuhaler, and Asmanex Twisthaler) was estimated using cascade impactor measurements and an in silico regional deposition model. These estimates were compared to direct measurements of regional deposition as provided by the TB filter mimic and an absolute filter placed downstream of the TB filter housing, representing the alveolar dose.

Results The two methods were shown to provide similar estimates of extrathoracic, tracheobronchial, and alveolar deposition, as well as total recovery of active pharmaceutical ingredients.

Conclusions Because of its design, the TB filter apparatus makes it possible to estimate regional deposition with inhalers directly using variable inhalation profiles without any additional equipment or changes to the experimental configuration. This method may be useful to expedite development of both innovative and generic drug products as it provides regional respiratory tract deposition estimates using fewer resources than existing methods.

KEYWORDS In vitro in vivo correlation · Pharmaceutical aerosols · Tracheobronchial · Alveolar

INTRODUCTION

Obtaining in vivo regional deposition measurements of inhaled aerosols directly in identified anatomical structures throughout the lungs remains an elusive goal, in part because it demands spatial and temporal imaging resolution that is beyond current abilities (1,2). Despite these challenges, Usmani et al. (3) demonstrated that targeted regional lung deposition of albuterol in the conducting airways improved therapeutic response relative to a similar dose depositing more deeply in the lung. Conversely, in situations involving occupational exposure to hazardous aerosols, localized deposition may lead to increased severity of adverse outcomes. Indeed, Schlesinger & Lippmann (4) pointed out that areas in the lung predisposed to increased particle deposition are also those areas most likely to see the onset of cancer. These examples highlight the importance of estimating regional deposition in the lungs, be it for optimizing therapeutic outcomes or for toxicology studies related to environmental aerosol exposure.

Particle size and inhalation flow rate are the two external variables that most strongly determine the eventual deposition site of the inhaled aerosol particles. During tidal breathing of ambient aerosols at rest, inhalation flow rate is set by metabolic need, so that to assess risks of exposure to

✉ Warren H. Finlay
warren.finlay@ualberta.ca

¹ Department of Mechanical Engineering, University of Alberta, Edmonton, Alberta, Canada

² 10-293 Donadeo Innovation Centre for Engineering, University of Alberta, 9211 116 Street, Edmonton, AB T6G 1H9, Canada

³ Proveris Scientific Corporation, Hudson, Massachusetts, USA

atmospheric aerosols the single most important variable is the size distribution of the aerosol. With knowledge of the size distribution of the particles in question, *in silico* deposition models can be used to predict the average dose that would deposit in the lungs or specific regions therein. Alternatively, a sampling device can be used to provide exposure estimates, assuming particles are captured with the same efficiency that they are expected to deposit in the body. Koehler et al. (5) describe a sampler that uses polyurethane foam as a filter medium to mimic deposition in the respiratory tract (inclusive of the nasal airway) for an average adult under light exercise breathing conditions (6). This sampler was shown to provide a good estimate of the internal dose of metals associated with exposure to welding fumes and is a step forward from common measurement methods that simply provide a measurement of ambient concentrations and particle size (7). This sampler was further developed by Koehler & Volckens (8) to include multiple filtration stages composed of polyurethane foams and nylon screens representative of the three regions of the respiratory tract, i.e., the extrathoracic, tracheobronchial, and alveolar regions.

While these samplers show great promise in their intended field of occupational hygiene, they are not suitable for use with pharmaceutical aerosols primarily because of their use of a constant flow rate that differs from the expected actual inhalation flow maneuver. It is also not expected that these samplers can be scaled and used directly to mimic regional deposition of pharmaceutical aerosols because the sampler is explicitly designed to mimic tidal breathing deposition efficiencies. For tidal breathing it is known that a significant amount of aerosol is exhaled (9), but for most single breath inhalers the exhaled dose is nearly eliminated due to deposition occurring during breath holding. Furthermore, assay of pharmaceutical ingredients may be difficult when using polyurethane and nylon substrates due to solubility of the substrate in solvents used for assay, resulting in interfering signals of dissolved pharmaceutical ingredients and dissolved substrate.

For estimating regional deposition of pharmaceutical aerosols, the inhalation flow rate generated through the device is of critical importance. As for all aerosols, this flow rate plays a major role in determining deposition efficiencies throughout the respiratory tract, but it is also the source of energy for aerosolizing and deagglomerating the powder contained in passive dry powder inhalers (DPIs). This relationship introduces a dependence of inhaler performance on inhalation maneuvers (flow rates vs. time) and further complicates the dependence of regional deposition on inhalation flow rate, necessitating direct testing of these inhalers using the inhalation maneuvers that patients are expected to perform during actual usage.

Currently, the preferred experimental setup designed to provide quantitative *in vitro* predictions of inhaler performance involves placing a cascade impactor downstream of

an extrathoracic airway model; if the extrathoracic airway model accurately mimics extrathoracic deposition, then the aerosol classified by the impactor represents the total lung dose and can be divided into regional deposition estimates by applying *in silico* deposition models (10). While in theory, this methodology can generate helpful insights into inhaler performance, it has many disadvantages. First, cascade impactors must operate at a constant flow, which makes testing inhalers with realistic breath profiles more complicated. While this problem can be overcome in large part by using mixing inlets and providing a bias flow to the impactor in order to generate time-varying flow through the inhaler (11–13), upper limits on inhalation flow rates are still imposed. More important is the issue of the resources required to perform cascade impactor experiments. If an experimenter is using the Next Generation Impactor (NGI), the aerosol is classified into seven size stages (eight if the pre-separator is used); each stage must be collected and assayed individually to determine the mass of aerosol in each size bin. If regional deposition estimates are desired, this size distribution data must then be coupled with a regional deposition model calculation before a final result can be reached. This procedure is so involved that a well trained laboratory analyst can only complete 1–2 cascade impactor measurements in a single work day, which precludes high volume testing. Using fewer stages in cascade impactor measurements (Fast Screening Impactors [FSI] or Abbreviated Impactor Measurements [AIM]) has been suggested to alleviate some of the resource burden associated with these measurements. However, such experiments still have the same upper limits on inhalation flow rates imposed by the highest calibration flowrate of the impactor, and require the same complex experimental method to test with realistic breath profiles. Moreover, the decreased resolution of the size distribution data may degrade the accuracy of regional deposition estimates.

Recently, Tavernini et al. (14) presented a filter that could be used to provide regional deposition estimates without the use of cascade impactor measurements. This filter was shown to have a filtration efficiency similar to predicted tracheobronchial (TB) deposition for a wide range of particle sizes and flow rates. The authors suggest the filter can be used downstream of an extrathoracic airway model and upstream of an absolute filter, the latter collecting any aerosol passing through the TB filter. The two filters separately capture the expected tracheobronchial and alveolar dose (assuming that there is no exhaled dose). It was not shown whether this filter functions as intended with pharmaceutical powder aerosols, since Tavernini et al. examined only the filtration efficiency of their TB filter sampling from a chamber containing laboratory-generated oil aerosol.

For DPI aerosols, a complicating issue is the electrostatic charge state of the particles exposed to the TB filter. It is known that particles emitted from DPIs can carry

considerable bipolar charge (15). Charged particles were not considered in the development of the Tavernini et al. (14) TB filter. Traditional methods for evaluating inhaler performance also do not take particle charge into consideration, and the effect that aerosol charge has on deposition in the lungs remains an area of study. Majid et al. (16) implemented electrostatic deposition in a stochastic lung deposition model and found TB deposition was enhanced by approximately 10% for one-micron and sub-micron sized particles inhaled at 30 L/min, while enhancement in the alveolar region was approximately 20%. The authors also compared deposition calculated at 18 and 50 L/min and found that at higher flow rates the enhancement was reduced in the TB region but increased in the alveolar region. Flow rates generated with the use of single breath inhalers are often higher than the authors studied, indicating TB deposition enhancement may be insignificant for those applications. Similar results were reported by Koullapis et al. (17), who employed computational fluid and particle dynamics to investigate the effects of particle charge on deposition in a realistic geometry of the human respiratory tract inclusive of the mouth-throat to the seventh generation of the lungs. At a flow rate of 60 L/min (the highest investigated in that study) deposition in the domain was nearly independent of particle charge for 2.5 μm particles and increased from about 20% to 30% for 1 μm particles. The authors show that for a flow rate of 15 L/min the deposition enhancement occurs primarily in the extrathoracic region, but they do not specify if this is the case at higher flow rates. Nevertheless, these two studies show that for pharmaceutically relevant particle sizes and inhalation flow rates, deposition in the tracheobronchial airways is largely independent of particle charge for charge levels and flow rates expected with pharmaceutical aerosols.

By contrast, particle charge could have major effects on the filtration efficiency of the Tavernini et al. (14) TB filter, since it is comprised of two layers of stainless-steel mesh. The square pores of the steel mesh are $\sim 30 \mu\text{m}$ wide, so that particles passing through the filter come into close proximity to the filter fibres. These distances are an order of magnitude smaller than even the final generation of the alveolar region, while the tracheobronchial region terminates with bronchioles approximately 600 μm in diameter (18). Since the fibres of the Tavernini et al. (14) TB filter are electrical conductors, image charges will readily form in the presence of a nearby charged particle, causing large electrostatic forces and thus higher filtration efficiency. While particle charge may not have a significant effect in the tracheobronchial region of the lungs in vivo, it may cause significant departure from the designed filtration efficiency of the Tavernini et al. idealized TB filter. This issue could be resolved by neutralizing the aerosol before exposing it to the TB filter.

In the present work, we adapt the TB filter as previously described by us (14) to include an electrostatic neutralizer and

an Alberta Idealized Throat inlet, and we demonstrate the ability of this combined apparatus to fractionate in vitro lung dose into tracheobronchial and alveolar regional deposition estimates for dry powder inhaler aerosols.

METHODS

Neutralizer Design

A custom bipolar ion source was designed to allow neutralization of inhaled pharmaceutical aerosol formulations prior to their passage through a filter that mimics TB deposition. Since the intent of the present TB filter device is to enable direct testing of inhalers with physiologically realistic inhalation profiles, the ion source must be integrated into the TB filter apparatus to rapidly neutralize aerosol after it exits the extrathoracic airway model before traversing the TB filter media. The internal volume must be minimized so that the aerosol emitted by the inhaler is exposed to the TB filter at an appropriate time in the breath inhalation maneuver.

An estimate for the maximum required ion concentration can be made by considering one of the most highly charged dry powder inhalers, the Pulmicort Turbuhaler (15). A total charge is assigned to each bin of the particle size distribution reported by Ruzycki et al. (10) by multiplying mass by charge-to-mass ratios reported by Yu et al. (15). The number of ions needed to neutralize the aerosol can then be determined by summing the total charge and dividing by the elementary charge. While Ruzycki et al. reported mass as a function of particle size for five actuations of a 200 μg per dose budesonide Turbuhaler, we chose not to divide the number of ions by five in order to extrapolate a worst case ion requirement. An ion concentration can then be determined by identifying the volume of the aerosol bolus. The emission kinetics of DPIs remains an area of study but depends on the device type, powder formulation, and inhalation maneuver (19). For the fastest emptying device studied by Dorosz et al., the bulk of aerosol appears to be emitted in as little as 0.4 s after only 0.1 s of inhalation, giving an aerosol bolus of about 400 mL for the flow profile used by Ruzycki et al. (10). Assuming that the aerosol is evenly distributed throughout the bolus leads to an estimate for an ion requirement of approximately 1.9×10^8 ions/mL to neutralize the aerosol. Note that this value represents only the ions required to neutralize the aerosol. In actuality an excess of ions is required since neutralization is not expected to be 100% efficient.

The ion requirement found with this approach happens to be very similar to the requirement reported by Hinds & Kennedy (20), who demonstrate that the radioactive source required to provide such an ion concentration is enormous. However, the authors also demonstrate the ability of a custom-made corona discharge ion generator to almost

entirely neutralize a unipolarly charged aerosol in their application. Their ion generator employs direct current applied to preferentially sized electrodes in order to generate the desired polarity of corona. For our application, 60 Hz alternating current (AC) was used to generate both polarities of ions, albeit at opposite phases of each AC cycle rather than simultaneously.

Bearing in mind the above considerations, we designed and built a custom ion generator to incorporate into the TB filter housing. A simple AC high-voltage source was built using a 10 kV transformer (2721-628G; Allanson International, Markham, Canada) which uses standard 120 V 60 Hz input to excite the secondary coil. Benchtop experimentation led to an electrode design in which one high-voltage lead was attached to an internally serrated stainless-steel ring, with the second high-voltage lead attached to a cylinder centred within the ring. Corona discharge was observed to form on each point of the serrated ring, emitting ions and creating an annular region of high ion concentration. Passing charged aerosol through this annulus provides the desired neutralization. To do so, however, necessitated redesigning the TB filter housing of Tavernini et al. (14) from a simple conical expansion to a more complex annular shape. This alteration is acceptable so long as the face velocity of the filter is maintained. The filter face velocity is the lowest velocity region in the experiment, making it also the ideal location to neutralize the aerosol. Changing the filter to an annular shape (while maintaining the face area) allows the annular ion-generating region to be placed directly upstream of the TB filter.

This design change was also inspired by the potential for the laryngeal jet (21,22) to persist into the TB filter housing and thereby cause non-uniform face velocity and thus off-spec filtration due to the previously mentioned dependence of filtration efficiency on face velocity. By introducing an abrupt expansion in the filter housing, the jet is forced off the anterior wall rather than remaining attached due to the Coanda effect. After rapid expansion from the extrathoracic model outlet, the free jet impinges on the top of the annular core to further distribute the energy of the jet into the bulk flow, allowing relatively uniform flow down the annular gap towards the TB filter. Since the jet impinges on the top of the annular core it is assumed that the largest particles remaining in the flow will be deposited here, so a collection dish was incorporated into the design at this location (herein referred to as the flow disruptor plate).

Figure 1 shows the details of the TB filter apparatus redesigned to an annular flow channel. The housing includes a centrally located 16 mm-diameter inlet which is the attachment point for the extrathoracic geometry to interface. This small diameter section then expands rapidly at a 60° expansion angle to a diameter of 75 mm. Axially aligned with the inlet is the annulus core, the top of which begins

approximately 30 mm in the axial direction from the onset of the expansion region of the inlet. The annulus core is a 45 mm-diameter cylindrical assembly; the top (flow disruptor) has a collection dish with 5 mm-tall walls and an inner diameter of 33 mm that is electrically grounded through connections inside the core. Teflon parts insulate the flow disruptor plate and the rest of the assembly from the “core electrode,” which is electrically connected to a lead extending outside the neutralizer. The core electrode has an axial length of 15 mm and an outer diameter of 45 mm. Across the annular gap, the corona electrode ring is axially centred relative to the core electrode; it is made of 0.003” (0.08 mm) thick 304 stainless steel and has 60 round serrations forming sharp points or “teeth” that serve as corona onset locations. These teeth are separated from the core electrode by 17 mm. The TB filter is located 42 mm downstream of the corona electrode ring. Each layer of the TB filter mesh (SV-26/25tw, SV-34/30tw; ASADA MESH Co., Osaka, Japan) is spot-welded between 1 mm-thick stainless steel rings, which supports the filter layers. The annular filtering region has an outer diameter of 75 mm and an inner diameter of 45 mm. These dimensions provide a filtering area equivalent to the previously described (14) 60 mm-diameter disk filters. Upon traversing the TB filter, the fluid region returns at a 45° draft angle to an internal pipe flow with a diameter of 18 mm. This is the exit of the TB filter housing where a final filter can be connected to capture the remaining particles representative of the alveolar dose. The internal dead space from the beginning of the inlet to the TB filter is 310 mL, and the total dead space of the entire housing 488 mL. See Fig. 1 for a depiction of how the sub-assemblies of the apparatus are assembled for use.

In Vitro Inhaler Performance

We obtained regional deposition estimates of four commercially available DPIs delivering different active pharmaceutical ingredients (APIs). Each device differs in either its metering mechanism, use of carrier particles (or not), or resistance to flow through the device. Inhalers tested included Onbrez Breezhaler (Lot SWN96; Novartis Pharmaceuticals Canada Inc., Dorval, Canada), Flovent Diskus (Lot W94G; GlaxoSmithKline Inc., Mississauga, Canada), Pulmicort Turbuhaler (Lot PAVE; AstraZeneca Canada Inc., Mississauga, Canada), and Asmanex Twisthaler (Lot T032728; Merck Canada Inc., Kirkland, Canada). Details of each device are listed in Table I. Inhalation profiles were different for each device because of differences in device resistance. Delvadia et al. (23) measured in vivo profiles generated through different resistance inhalation flow cells and provided the method for selecting appropriate inhalation profiles for in vitro inhaler performance testing that we follow here. The inhaler resistance defines the peak inspiratory flow rate (PIFR). We used the 50th percentile PIFRs expected to be

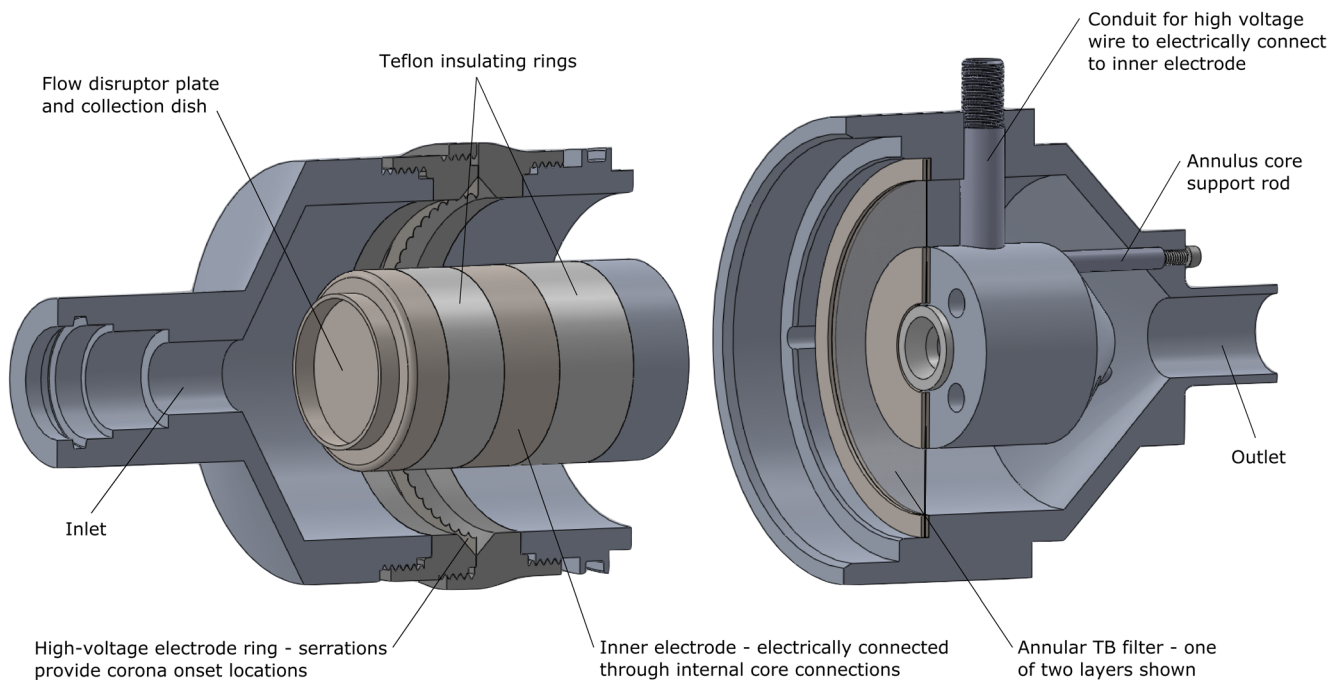


Fig. 1 Partial section view of the annular neutralizer + TB Filter assembly. Flow is from left to right. In operation the left-most pieces are in contact with the top of the TB filter.

generated after professional instruction (Eq. 5 in [23]), except in the case of the Breezhaler, which by this formula would be tested with a PIFR higher than the maximum allowed when using the NGI. The time at which the PIFR was generated (t_{PIFR}) and the total volume inhaled (V) were independent of inhaler resistance and were therefore constant for all devices. We used $t_{PIFR} = 0.49$ s and $V = 2.7$ L, which are the 50th percentile values for mixed-gender data [23]. The shape of the breath profile is similar for all inhalers and is made up of two sinusoidal quarter waves. The first quarter wave is the “ramp up” period where inhalation flow rate quickly accelerates to PIFR. The second quarter wave is the majority of the breath from t_{PIFR} to the end of the breath, t_{total} , which is set by the total volume inhaled (Eq. 10 in [23]). The unique inhalation parameters for each inhaler are also listed in Table I.

Two different experiments were performed (with $n = 5$ measurements each) for each inhaler with these inhalation profiles. One experiment involved direct measurements of

the TB filter device performance downstream of an Alberta Idealized Throat. The other involved cascade impactor measurements to characterize the inhaler particle size distribution for use in a regional deposition model (see next section).

Inhaler Specific Regional Deposition Estimates

Regional lung deposition estimates for each inhaler were established based on cascade impactor measurements, the results of which were used as input for an in silico regional deposition model. The method used very closely follows the method used by Ruzycki et al. (10), so we describe it only briefly here. For the upstream mouth-throat inlet, we used the Alberta Idealized Throat (AIT). The inhaler being tested was coupled to the inlet of the AIT with a 3D-printed custom adapter unique to that inhaler type, providing an airtight seal and ensuring consistent and proper orientation of the inhaler relative to the AIT. A Mixing Inlet (MSP Corporation,

Table I List of inhalers studied, physical attributes, and inhalation pattern defining parameters.

Inhaler	API	Doses	Label Claim [μg of API]	Carrier Particles	Metering Mechanism	Device Resistance, R [$\text{kPa}^{0.5}/(\text{L}/\text{min})$]	PIFR [L/min]	t_{total} [s]
Onbrez Breezhaler	Indacaterol maleate	30	97	Lactose anhydrous	Capsule	0.0212	100.0	2.36
Flovent Diskus	Fluticasone propionate	60	250	Lactose	Blister	0.0273	87.7	2.90
Pulmicort Turbuhaler	Budesonide	200	200	None	Hopper	0.0473	59.5	4.28
Asmanex Twisthaler	Mometasone furoate	60	400	Lactose monohydrate	Hopper	0.0302	81.3	3.13

API = Active Pharmaceutical Ingredient, PIFR = Peak Inspiratory Flow Rate, t_{total} = breath duration

Shoreview, MN, USA) downstream of the AIT enabled use of time-varying inhalation profiles through the inhaler/extrathoracic model while providing a constant flow of 100 L/min (volumetric) to an NGI with a pre-separator stage (MSP Corporation). An inhalation profile was generated by a custom-built breathing machine that draws from the supply to the mixing inlet. The resulting deficit in makeup air causes the NGI to pull air through the AIT and inhaler. Flow rates were monitored using mass flow meters (4040 and 4043; TSI Incorporated, Shoreview, MN, USA) and the volumetric flow generated through the inhaler was calculated as described by Ruzycski et al. (10) using a LabVIEW program (LabVIEW Professional Development System 2017; National Instruments, Austin, TX, USA). This experimental configuration is demonstrated in Fig. 2a.

The cascade impactor data obtained from the above experimental configuration represent the total lung dose, provided that the appropriate fraction of particles is removed in the AIT. One mechanism that can cause decreased collection efficiency in the AIT is particle bounce, where a particle that would otherwise be deposited on the extrathoracic airway wall instead rebounds back into the flow. This mechanism artificially inflates the mass of API reaching the lungs but is also difficult to detect. Zhou et al. (24) investigated the difference in particle collection of liquid droplets vs. solid particles with and without coating the walls of extrathoracic models with silicone lubricant fluid. They suggest that for particles <10 μm , bounce should not be a concern when wall coatings are used. However, for particles >10 μm some bounce may occur and is evident by the plateau in deposition observed for polystyrene latex particles around 90% efficiency, which does not occur for oleic acid droplets. While few of these relatively massive particles may bounce through the AIT, they carry significant mass. Conveniently, when using the pre-separator at 100 L/min the cut-point is 10 μm , meaning that particles collected in the pre-separator are 10 μm and larger and thus could be those subject to bouncing through the AIT. Therefore, in the present work we add any mass detected on the pre-separator to that collected in the AIT and refer to these as the Upper Respiratory Tract fraction (URT). Thus, only the sized mass collected from the stages of the NGI are considered to contribute to the lung dose in this work.

Regional lung deposition estimates from NGI data were obtained using the regional deposition model presented by Javaheri et al. (25), which uses deposition efficiency equations for inertial impaction (26), sedimentation (27,28), and diffusion (29) to estimate total deposition in each generation of a symmetric lung model (30). In this lung model the trachea is represented by generation 0, the tracheobronchial (or conducting airway) region by generations 0–14, and the alveolar region by generations 15–23. This model was used to generate regional deposition estimate targets because an earlier version of the model has been validated against in vivo, single photon

emission computerized tomography (SPECT) data (31) and against planar gamma scintigraphy (32).

Extrathoracic deposition was not present in the in silico model, since it is already accounted for in the URT deposition noted above. Particle diameters used for evaluating deposition efficiencies were the geometric centres of the stage-bounding 50% collection efficiencies. Particle sizes were assumed to be constant, and hygroscopic effects were neglected. The model uses a constant flow rate to propagate a constant density aerosol through the lung generations; since we expect the aerosol to interact with the TB filter at approximately the PIFR, we adjusted the breath time in the in silico model so that the resulting average flow rate (inhaled volume divided by inhalation time) was equal to the PIFR used for that inhaler. A 10 s breath hold and 7 s exhalation were used for all inhalers (although the latter has little effect on our results since the breath hold reduces the exhaled aerosol to negligible amounts). Total inhaled volume was the same 2.7 L used in the TB filter runs described above. Tracheobronchial deposition was then estimated by summing the calculated particle deposition in generations 0–14. Alveolar deposition was taken to be the total NGI mass less the TB estimate, as this approach best aligned with our experimental method, in which there is no exhaled fraction of aerosol.

These estimates provided target regional lung deposition values for the TB filter device to achieve. Because of variability in the conception of different regional deposition models and inter-subject variability known to exist in vivo, these targets should be considered approximate.

TB Filter Performance

The performance of the TB filter with the neutralizer device was measured directly. The device was built such that the AIT outlet interfaced directly with the device inlet. A final filter (H8–6301; KEGO Corporation, London, Canada) installed at the outlet of the TB filter housing collected all remaining particles. This filter was in fluid connection to a mass flow meter and the breathing machine that directly generated the appropriate inhalation profile through the entire apparatus. This configuration is shown in Fig. 2b. The inhalation profile was calibrated to match the profile generated during the NGI experimental runs. The API landing in the AIT model and on the flow disruptor plate, on the TB filter, and on the final filter directly give the regional deposition estimates (URT, TB, and alveolar, respectively), which are then compared to the estimates provided by the in silico modeling of the NGI data.

Experimental Procedure

On each day of experimentation the ambient conditions were recorded. Pressure was recorded from one of the flowmeters while the apparatus was open to the atmosphere and under no

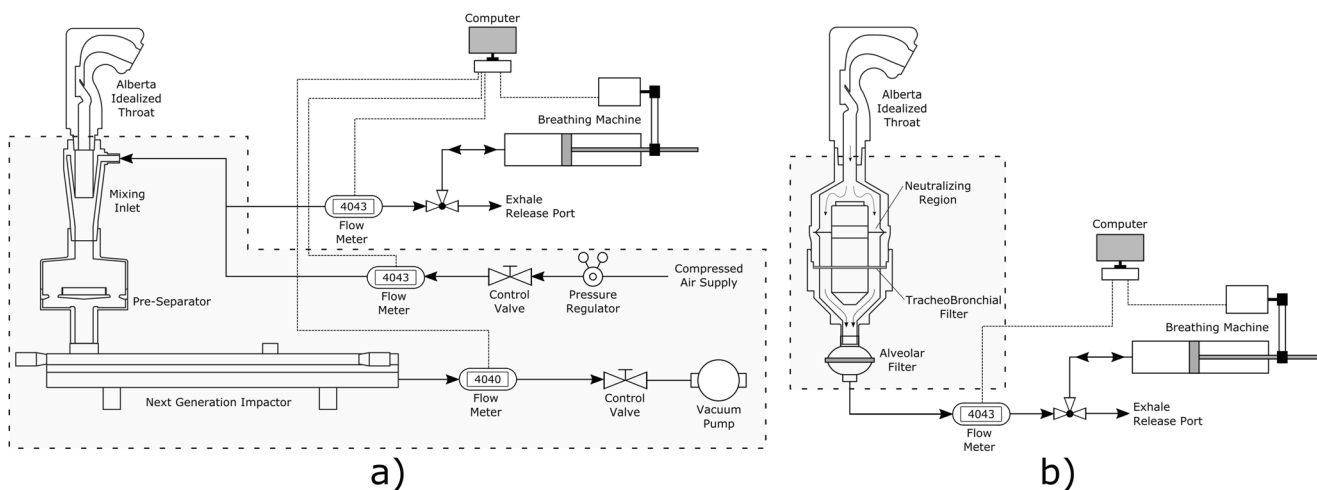


Fig. 2 Schematic diagrams indicating the experimental apparatus for a) cascade impactor measurements or b) the regional deposition filter apparatus. Equipment enclosed by a dashed box indicates the difference in equipment needed for each experiment and highlights the simplicity of the regional deposition filter experiment.

flow conditions. Temperature and relative humidity were measured using a digital hygrometer/thermometer (MI70 Measurement Indicator and HMP75B Humidity and Temperature Probe; Vaisala, Vantaa, Finland). Ambient conditions (temperature, pressure, and relative humidity) ranged from 21 to 23°C, 90.7–94.5 kPa, and 13–26%.

For all experiments the interior surfaces of the clean, dry AIT were coated with silicone release spray (Molycote 316; Dow Corning, Midland, MI, USA). This spray was also used on all stages of the NGI impactor plates and the pre-separator impactor plate. The propellant/solvent was allowed to evaporate for a minimum of 15 min before the equipment was assembled. A specialized 3D-printed adapter for the inhaler being tested was affixed to the AIT inlet and the appropriate inhalation profile loaded into the breathing machine. For NGI runs, the vacuum pump pulling flow through the impactor was turned on and the flow set to 100 L/min. The makeup air supply to the mixing inlet was then adjusted to match, producing zero flow at the AIT inlet. For runs with the TB filter device, no flow monitoring/matching was required. The only additional preparation step with the TB filter setup was to place a small amount of solvent on the flow disruptor plate. Using the assay solvent here eliminates bounce (similar to a liquid impinger) and makes for simple and effective collection of any API landing on this plate.

With the apparatus assembled and ready for the inhaler to be tested, the inhaler was primed and loaded following the directions in the leaflet supplied with the inhaler. When the dose was ready to be inhaled, the inhaler was brought to the AIT and held firmly in place. The breathing machine was actuated and a single inhalation maneuver was generated through the device. For TB filter runs, the neutralizer was manually switched on just prior to generation of the inhalation and switched off when the machine stopped. The inhaler was then removed from the adapter at the AIT inlet. Valves in the

system piping allowed the piston of the breathing machine to return to the starting position with the resulting exhalation being directed out of a release port rather than through the system. In the case of the Breezhaler, the capsule was inspected to ensure it was completely empty; if powder remained, the inhalation procedure was repeated as per the product leaflet instructions. Subsequent doses (as per Table I) were delivered following the same procedure, in accordance with all product leaflet instructions.

When the predetermined number of doses had been delivered, the collection surfaces of the components were washed with HPLC-grade methanol ensuring API was collected in full. The AIT was washed twice with 10 mL, NGI collection stages were washed with 5 mL, and the pre-separator and flow disruptor plate were also washed with 5 mL except in the case of the Twisthaler runs, where 10 mL was used due to increased deposition. The stainless-steel TB filters were washed twice with 10 mL of methanol, while the fibrous alveolar filters were washed with a total of 25 mL divided into three parts. The mass of API contained in each sample was quantified via ultraviolet light absorbance relative to a series of prepared standards. Absorption was measured using a UV-Vis spectrophotometer (Cary 8454; Agilent, Santa Clara, CA, USA) at 236, 243, 248, and 260 nm for fluticasone propionate (Diskus), budesonide (Turbuhaler), mometasone furoate (Twisthaler), and indacaterol maleate (Breezhaler), respectively. Absorbance was always measured relative to a blank sample prepared exactly as the sample would be collected in the experiment, to eliminate any interference of UV-absorbing ingredients from silicone release spray or dissolved plastics. For each inhaler, the above procedures were repeated five times for each configuration to provide a measure of repeatability. Statistical comparisons of regional deposition estimates were performed using the two-tailed, unpaired student's *t* test in Microsoft Excel 2016 (Microsoft, Redmond, WA, USA).

RESULTS

The results of characterizing the inhalers with the NGI are given in Table II. Similarly, the results of testing the same inhalers with the regional deposition filter apparatus are given in Table III. In silico regional deposition estimates arising from NGI data are presented in Table IV alongside the in vitro regional deposition estimates from the TB filter and neutralizer apparatus.

Since the masses collected on the flow disruptor plate and pre-separator were similar, it is safe to assume the aerosol classified by the NGI is representative of the aerosol travelling through the filter. Indeed, the total lung dose is the same for each experimental configuration ($p > 0.05$). Excluding the flow disruptor and pre-separator dose from the tracheobronchial deposition estimates results in a pure comparison of the TB filter's ability to mimic the in silico deposition model. Comparison of the regional lung deposition between the two approaches can be done in terms of mass, fraction of recovered dose, or fraction of lung dose estimated to deposit in each location; all three such comparisons are shown in Fig. 3.

DISCUSSION

The aforementioned comparisons of regional deposition estimates show that the TB filter satisfactorily mimics the estimated tracheobronchial deposition given by a regional deposition model applied to the sized mass as measured by cascade impaction. In some cases, the TB filter appears to capture slightly more mass than predicted by the regional deposition model, a discrepancy that could be due to incomplete neutralization or else a tendency of the filter to capture slightly more mass than is predicted by the model used here. Given the variations in predictions by different in silico models (14) and the large in vivo variability, we believe these differences are acceptable.

Explicit verification of the in vitro TB filter results against in vivo regional deposition measurements is beyond the scope of this work, and in general establishing in vitro in vivo correlations is a complex (1,32,33) and ongoing area of work. However, the TB filter regional deposition estimates can be indirectly compared with in vivo regional deposition measurements through consideration of the deposition models the filter has been shown to agree with. When the filter was first developed (14), it was shown to have a filtration efficiency which closely mimics regional deposition estimated by models based on in vivo measurements (6,34). Further, in the present work the TB filter gives reasonable agreement to the NGI data interpreted through a well established model (10,25,35) which has been shown previously to agree with in vivo data (31).

As expected, Table IV shows there is generally no significant difference in URT deposition since the AIT is used in

both experimental configurations and the inhalation pattern is the same. Though URT is statistically different for the Asmanex Twisthaler, the small difference is aligned with the statistically significant difference in total recovered API; these differences were not detected for any other inhaler.

While the ability of the custom ion generator to neutralize the test aerosol was not directly measured, it was indirectly assessed by comparing the mass of budesonide recovered from the TB filter in runs where the neutralizer was not powered. These experiments were merely exploratory in scope, so a full data set is not presented here. However, for a Pulmicort Turbuhaler (a different individual inhaler device than presented in Tables 2–4) the TB filter mass decreased from $101.4 \pm 16.7 \mu\text{g}$ when the neutralizer was not used to $47.4 \pm 14.0 \mu\text{g}$ when the neutralizer was powered at 10 kV (for 3 actuations per run, $n = 5$ runs). This represents a reduction from $23.3 \pm 2.1\%$ of the recovered dose to $10.3 \pm 2.1\%$. Additionally, we briefly investigated if neutralizing the aerosol entering the NGI could affect the measured size distribution and ensuing regional deposition estimates. To make this comparison, we positioned the neutralizer housing upstream of the mixing inlet and NGI and performed runs with and without voltage applied to the neutralizer. We used the Turbuhaler in this investigation since we expected its emitted aerosol to be the most charged of the inhalers studied here (15), and thus potentially exhibit the largest difference in comparison with its neutralized size distribution. Three runs using five actuations of the inhaler were performed with the neutralizer powered and with the neutralizer off. For the charge levels associated with the Turbuhaler, and the neutralization levels given by our custom neutralizer, no significant difference ($p > 0.1$) in particle size distribution or regional deposition estimates was observed.

Also being monitored during those exploratory experiments was the amount of API collected from a swab of the interior walls upstream of the TB filter in the neutralizing region. With the neutralizer off, $19.6 \pm 4.7 \mu\text{g}$ was recovered from the walls, but with the neutralizer at 10 kV this increased to $53.8 \pm 17.3 \mu\text{g}$, or an increase from $4.5 \pm 0.9\%$ of recovered mass to $11.5 \pm 1.7\%$. Further experimentation indicated that powering the neutralizer with 5 kV reduced wall losses to only $3.3 \pm 0.5\%$ of the recovered dose while still adequately neutralizing the aerosol. This finding led to using the neutralizer with a potential difference of 5 kV in all further experiments. Wall losses were not monitored further as they were considered acceptable. Indeed, total recovery was consistent between all runs when comparing NGI runs and those using the TB filter device, indicating that the wall losses were similar in the two experiments.

While the total recovered dose was not of primary interest, in this research it serves as a measure of the integrity of the experiment being performed. For the Breezhaler, Diskus, and Twisthaler devices total recovery as a percent of the label

Table II Amount of API collected from each collection surface for runs using the NGI.

	Breezhaler	Diskus	Turbuhaler	Twisthaler
AIT (μg)	88.2 \pm 6.0	318.3 \pm 19	248.1 \pm 13.3	343.9 \pm 32.6
PS (μg)	2.6 \pm 2.4	0.0 \pm 0.0	70 \pm 20.7	260.1 \pm 29.9
NGI Stage 1 (μg)	5.9 \pm 0.4	9.7 \pm 2.7	18.4 \pm 2.5	12.5 \pm 2.9
NGI Stage 2 (μg)	16.6 \pm 0.5	26.7 \pm 0.9	44.5 \pm 5.2	18.3 \pm 2.3
NGI Stage 3 (μg)	19.5 \pm 0.5	26.9 \pm 2.3	51.2 \pm 3.1	21.2 \pm 2.1
NGI Stage 4 (μg)	14.6 \pm 0.8	19.7 \pm 2.1	53.8 \pm 2.8	21.0 \pm 1.8
NGI Stage 5 (μg)	3.2 \pm 0.7	1.2 \pm 1.5	23.3 \pm 1.2	8.3 \pm 0.8
NGI Stage 6 (μg)	0 \pm 0	0 \pm 0	0 \pm 0	0 \pm 0
NGI Stage 7 (μg)	0 \pm 0	0 \pm 0	0 \pm 0	0 \pm 0
NGI Stage 8 (μg)	0 \pm 0	0 \pm 0	0 \pm 0	0 \pm 0
MMAD (μm)	2.95 \pm 0.06	3.16 \pm 0.10	2.63 \pm 0.10	2.84 \pm 0.10
GSD	1.81 \pm 0.02	1.76 \pm 0.04	1.94 \pm 0.02	2.02 \pm 0.07

Data is shown as average \pm standard deviation for $n = 5$ runs. AIT = Alberta Idealized Throat, PS = Pre-Separator, NGI = Next Generation Impactor, MMAD = Mass Median Aerodynamic Diameter, GSD = Geometric Standard Deviation

claim was $79.5 \pm 4.1\%$, $79.8 \pm 3.3\%$, and $87.7 \pm 3.1\%$, respectively. However for the Turbuhaler, the recovery dropped to $50.4 \pm 3.3\%$ of label claim. The low recovery when using the Turbuhaler was surprising when considering the satisfactory recovery of the other inhalers. It is not, however, without precedent. Hill & Slater (36) found an emitted dose from the Turbuhaler of $46.0 \pm 14.6\%$ of the label claim, while Hindle & Byron (37) found similarly low recovery and showed significant variability between devices. Presumably, the amount of API recovered for each inhaler tested is indicative of the emitted dose for that inhaler, which is less than the nominal dose.

The API collected from the pre-separator and the flow disruptor plate allows for some interesting speculation. The pre-separator is a carefully designed impactor stage intended to operate at a constant flow rate and to provide a sharp change in deposition efficiency (otherwise known as a cut-point). The flow disruptor plate is substantially different in that it operates under variable flow rate defined by the inhalation pattern used. For this reason, a calibrated cut-point cannot be defined. Despite this fundamental difference, a similar amount of API was collected on the pre-separator and the flow disruptor plate for each inhaler. While the pre-separator was always operated at 100 L/min, the flow disruptor plate saw peak flow rates as low as 60 L/min while still

collecting a similar amount of API. Although it cannot be stated with certainty, it is likely that particles are sized similarly by the two and that the particles collected on these surfaces have bounced through the AIT and are relatively massive. This is supported by physical observations made during preliminary experiments with the Twisthaler before solvent was used on the flow disruptor plate. Originally, the disruptor plate was sprayed with the same silicone release spray used to reduce bounce in the AIT and on the impactor stages. Despite the use of this spray in the AIT and on the flow disruptor plate, exceptionally large particles were observed on the TB filter after experimentation. Since these particles were visible to the naked eye, we did not believe they could be avoiding contact with the flow disruptor. However, to investigate this possibility, solvent was placed in the flow disruptor plate and the experiment was repeated. The effects of this change were immediately visible as these large particles were no longer observed on the TB filter surface but instead were found in a pile in the solvent on the flow disruptor plate.

The notion that particle bounce is responsible for API being found on the flow disruptor plate and in the pre-separator is also supported by the variability observed between API recovery from the AIT versus the variability in URT deposition. Recall that URT deposition here is the sum of API recovered from the AIT and from the pre-separator or the flow

Table III Amount of API collected from each collection surface for runs using the TB filter and neutralizer device.

	Breezhaler	Diskus	Turbuhaler	Twisthaler
AIT (μg)	87.3 \pm 4.7	302.5 \pm 4.4	240.8 \pm 19.9	342.9 \pm 39.4
Flow Disruptor (μg)	4.3 \pm 0.6	0.0 \pm 0.0	64.7 \pm 16.9	293.1 \pm 44.0
TB Filter (μg)	29.9 \pm 4.8	31.9 \pm 4.2	56.8 \pm 7.8	35.9 \pm 3.8
Final Filter (μg)	36.2 \pm 2.2	60.7 \pm 4.6	136.1 \pm 14.3	45.7 \pm 4.7

Data is shown as average \pm standard deviation for $n = 5$ runs. AIT = Alberta Idealized Throat, TB = Tracheobronchial

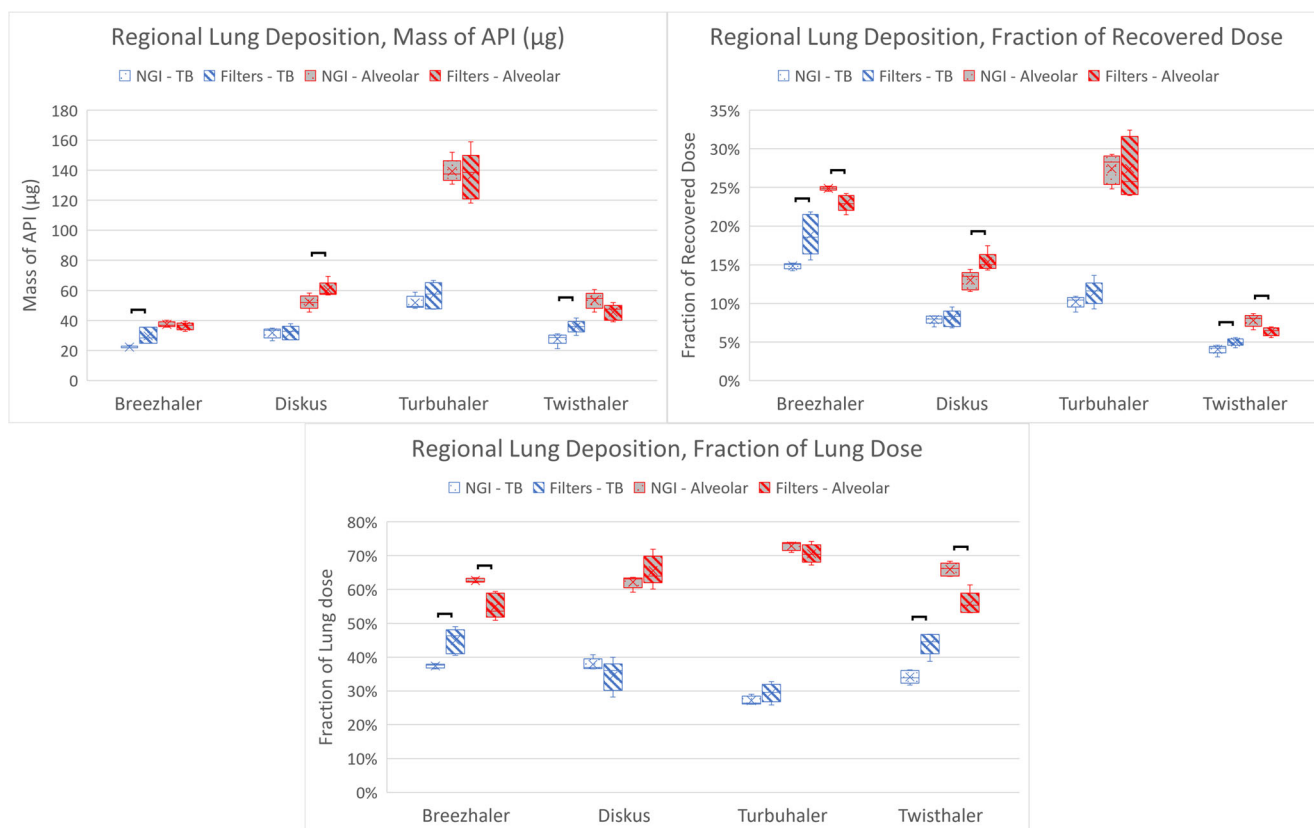
Table IV Regional deposition estimates arising from the two different experimental configurations; *in silico* regional deposition based on cascade impactor data vs. fully *in vitro* regional deposition filter device

	Breezhaler		Diskus		Turbuhaler		Twisthaler		
	NGI + RegDep	Filters	NGI + RegDep	Filters	NGI + RegDep	Filters	NGI + RegDep	Filters	
URT (μg)	90.8 \pm 3.6	91.7 \pm 4.2	318.3 \pm 17.3	302.5 \pm 4.0	318.2 \pm 27.2	305.5 \pm 32.0	604.0 \pm 10.5	* 636.1 \pm 18.3	
TB (μg)	22.4 \pm 0.6	* 29.9 \pm 4.4	31.9 \pm 2.8	31.9 \pm 3.8	51.9 \pm 3.6	56.8 \pm 7.1	27.8 \pm 3.1	* 35.9 \pm 3.4	
Alveolar (μg)	37.5 \pm 1.5	36.2 \pm 2.1	52.3 \pm 3.8	* 60.7 \pm 4.2	139.3 \pm 6.5	136.1 \pm 13.1	53.5 \pm 4.6	45.7 \pm 4.3	
Total (μg)	150.6 \pm 5.4	157.8 \pm 7.4	402.5 \pm 19.6	395.1 \pm 7.2	509.4 \pm 30.1	498.4 \pm 28.5	685.3 \pm 7.4	* 717.6 \pm 23.5	

URT Upper Respiratory Tract, TB Tracheobronchial, NGI Next Generation Impactor. RegDep = In silico Regional Deposition model of (Javaheri et al., 2013), * between values indicates statistically significant difference ($p < 0.05$)

disruptor plate (depending on the experimental configuration). Variability in URT deposition is reduced when compared to AIT deposition (see Table II, Table III, and Table IV) for the Twisthaler and Breezhaler. The amount of bounce occurring in the AIT for a given flow rate will depend on the AIT coating quality and the extent of deagglomeration occurring in the inhaler. For example, if slightly less coating is applied in a particular run more bounce may occur; however, if the inhaler powder deagglomerates well, the amount of bounce may decrease. Regardless of this interplay between coating quality and inhaler performance, if the pre-separator

or flow disruptor plate is catching these bouncing particles, there should be an inverse relationship between the mass collected on these surfaces and in the AIT. That is, if particles bounce through the AIT (thereby reducing mass collected in the AIT) they should be recovered from the pre-separator or flow disruptor, where mass will be increased. This trend is confirmed for the Twisthaler and Breezhaler by plotting the mass recovered in the AIT against the mass recovered from the pre-separator or flow disruptor plate, as shown in Fig. 4. This inverse relationship explains the reduction in variability of URT deposition relative to AIT deposition since URT

**Fig. 3** Various comparisons of the regional deposition estimates for each inhaler studied arising from cascade impactor measurements or direct measurements with the TB filter device. Overbar indicates statistically significant difference ($p < 0.05$).

deposition should be independent of bounce occurring in the AIT.

The converse is observed for the Turbuhaler (Fig. 5). However this difference could be explained by the lack of carrier particles used in this formulation. Since there are no large carrier particles, these particles are likely agglomerates of smaller particles of budesonide (38). While most of these particles will impact in the AIT, some do have the chance of traversing through and carrying significant mass with them. The positive linear relationship in Fig. 5 indicates that if more API is emitted from the inhaler in a particular run there is increased deposition in both locations, suggesting that these particles did not bounce through the AIT and could therefore be considered as TB deposition. This does not change the agreement between the two experiments; considering the pre-separator and flow disruptor plate mass as tracheobronchial deposition reduces URT deposition and increases TB deposition by nearly the same amount for the two experimental configurations.

These trends suggest that without further knowledge of the aerosol size distribution, the experimenter could identify whether mass landing on the flow disruptor plate should be considered URT or TB deposition by comparing the relationship between AIT and flow disruptor plate deposition.

CONCLUSIONS

The ability of a filter mimicking tracheobronchial deposition to collect the correct fraction of particles exiting the AIT has been demonstrated with commercially available dry powder inhalers. This filter provides a fast method to estimate in vivo regional lung deposition using in vitro inhaler testing. Electrostatic charge on the aerosol particles has the potential

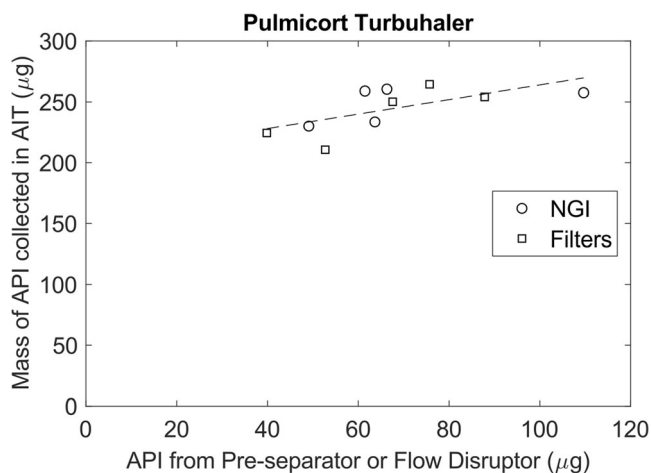


Fig. 5 Relationship between API mass collected in the AIT vs on the flow disruptor or pre-separator immediately downstream of the AIT for Pulmicort Turbuhaler. Series indicates the experimental configuration; line of best fit is for aggregate data ($R^2 = 0.43$).

to cause the TB filter to remove more particles than intended, but this issue was resolved by using an alternating current corona discharge ion generator integrated into the filter housing to quickly and adequately neutralize the aerosol just upstream of the filter. This apparatus can be used directly downstream of the AIT and has a small enough internal volume to allow direct testing of inhalers with the inhalation maneuvers expected to be performed by patients using the device. The apparatus presented here may be useful as a tool for inhaler product research and development.

Acknowledgments and Disclosures. This research was financially supported by Proveris Scientific Corporation and the Natural Sciences and Engineering Research Council of Canada (NSERC). The authors thank Dr. Milad Kiaee for

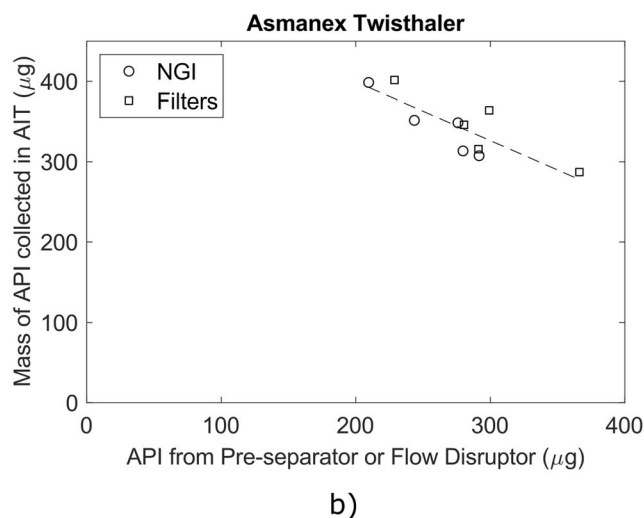
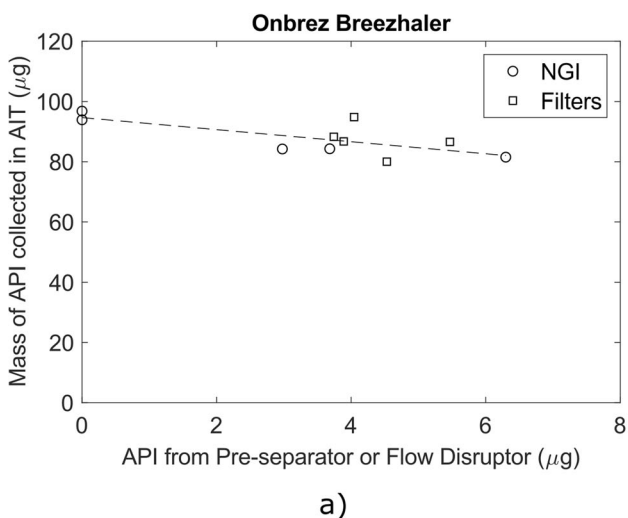


Fig. 4 Relationship between API mass collected in the AIT vs on the flow disruptor or pre-separator immediately downstream of the AIT for a) the Onbrez Breezhaler and b) the Asmanex Twisthaler. Series indicates the experimental configuration; line of best fit is for aggregate data (a) $R^2 = 0.52$, b) $R^2 = 0.69$

assistance with computational fluid dynamics investigation of the device design, and ASADA Mesh Company for supplying materials to construct the filter elements. Patents have been filed on the technology described in this work, which may financially benefit the authors. The research described in this manuscript was funded in part by Proveris Scientific Corporation.

REFERENCES

- Byron PR, Hindle M, Lange CF, Longest PW, McRobbie D, Oldham MJ, et al. In vivo-in vitro correlations: predicting pulmonary drug deposition from pharmaceutical aerosols. *J Aerosol Med Pulm Drug Deliv.* 2010;23(Suppl 2):59–69. <https://doi.org/10.1089/jamp.2010.0846>.
- Martin AR. Regional deposition: targeting. *J Aerosol Med Pulm Drug Deliv.* 2021;34(1):1–10. <https://doi.org/10.1089/jamp.2021.29033.am>.
- Usmani OS, Biddiscombe MF, Barnes PJ. Regional lung deposition and bronchodilator response as a function of β_2 -agonist particle size. *Am J Respir Crit Care Med.* 2005;172(12):1497–504. <https://doi.org/10.1164/rccm.200410-1414OC>.
- Schlesinger RB, Lippmann M. Selective particle deposition and bronchogenic carcinoma. *Environ Res.* 1978;15(3):424–31. [https://doi.org/10.1016/0013-9351\(78\)90123-8](https://doi.org/10.1016/0013-9351(78)90123-8).
- Koehler KA, Clark P, Volkens J. Development of a sampler for Total aerosol deposition in the human respiratory tract. *Ann Occup Hyg.* 2009;53(7):731–8. <https://doi.org/10.1093/annhyg/mcp053>.
- International Commission on Radiological Protection. Human respiratory tract model for radiological protection. A report of a task group of the International Commission on Radiological Protection. *Ann ICRP.* 1994;24:1–482.
- Newton A, Serdar B, Adams K, Dickinson LM, Koehler K. Lung deposition versus inhalable sampling to estimate body burden of welding fume exposure: a pilot sampler study in stainless steel welders. *J Aerosol Sci.* 2021;153:105721. <https://doi.org/10.1016/j.jaerosci.2020.105721>.
- Koehler KA, Volkens J. Development of a sampler to estimate regional deposition of aerosol in the human respiratory tract. *Ann Occup Hyg.* 2013;57(9):1138–47. <https://doi.org/10.1093/annhyg/met041>.
- Yang MY, Ruzycki C, Verschuer J, Katsifis A, Eberl S, Wong K, et al. Examining the ability of empirical correlations to predict subject specific in vivo extrathoracic aerosol deposition during tidal breathing. *Aerosol Sci Technol.* 2017;51(3):363–76. <https://doi.org/10.1080/02786826.2016.1262532>.
- Ruzycki CA, Murphy B, Nathoo H, Finlay WH, Martin AR. Combined in Vitro-in Silico Approach to Predict Deposition and Pharmacokinetics of Budesonide Dry Powder Inhalers. *Pharm Res.* 2020;37(10). <https://doi.org/10.1007/s11095-020-02924-7>.
- Chrystyn H, Safioti G, Keegstra JR, Gopalan G. Effect of inhalation profile and throat geometry on predicted lung deposition of budesonide and formoterol (BF) in COPD: an in-vitro comparison of Spiromax with Turbuhaler. *Int J Pharm.* 2015;491(1–2):268–76. <https://doi.org/10.1016/j.ijpharm.2015.05.076>.
- Finlay WH, Gehmlich MG. Inertial sizing of aerosol inhaled from two dry powder inhalers with realistic breath patterns versus constant flow rates. *Int J Pharm.* 2000;210(1–2):83–95. [https://doi.org/10.1016/S0378-5173\(00\)00569-X](https://doi.org/10.1016/S0378-5173(00)00569-X).
- Olsson B, Borgström L, Lundbäck H, Svensson M. Validation of a general in vitro approach for prediction of Total lung deposition in healthy adults for pharmaceutical inhalation products. *J Aerosol Med Pulm Drug Deliv.* 2013;26(6):355–69. <https://doi.org/10.1089/jamp.2012.0986>.
- Tavernini S, Kiaee M, Farina DJ, Martin AR, Finlay WH. Development of a filter that mimics tracheobronchial deposition of respirable aerosols in humans. *Aerosol Sci Technol.* 2019;53(7):802–16. <https://doi.org/10.1080/02786826.2019.1606414>.
- Yu J, Wong J, Ukkonen A, Kannosto J, Chan H-K. Effect of relative humidity on bipolar electrostatic charge profiles of dry powder aerosols. *Pharm Res.* 2017;34(8):1707–15. <https://doi.org/10.1007/s11095-017-2178-3>.
- Majid H, Madl P, Hofmann W, Alam K. Implementation of charged particles deposition in stochastic lung model and calculation of enhanced deposition. *Aerosol Sci Technol.* 2012;46(5):547–54. <https://doi.org/10.1080/02786826.2011.645957>.
- Koullapis PG, Kassinos SC, Bivolarova MP, Melikov AK. Particle deposition in a realistic geometry of the human conducting airways: effects of inlet velocity profile, inhalation flowrate and electrostatic charge. *J Biomech.* 2015;49(11):2201–12. <https://doi.org/10.1016/j.jbiomech.2015.11.029>.
- Finlay WH. The mechanics of inhaled pharmaceutical aerosols : an introduction: Academic Press; 2019.
- Dorosz A, Żaczek M, Moskal A. Dynamics of aerosol generation and release – dry powder inhaler performance considerations. *J Aerosol Sci.* 2021;151:105673. <https://doi.org/10.1016/j.jaerosci.2020.105673>.
- Hinds WC, Kennedy NJ. An ion generator for neutralizing concentrated aerosols. *Aerosol Sci Technol.* 2000;32(3):214–20. <https://doi.org/10.1080/027868200303740>.
- Heenan A, Matida E, Pollard A, Finlay W. Experimental measurements and computational modeling of the flow field in an idealized human oropharynx. *Exp Fluids.* 2003;35(1):70–84. <https://doi.org/10.1007/s00348-003-0636-7>.
- Johnstone A, Uddin M, Pollard A, Heenan A, Finlay W. The flow inside an idealised form of the human extra-thoracic airway. *Exp Fluids.* 2004;37(5):673–89. <https://doi.org/10.1007/s00348-004-0857-4>.
- Delvadia RR, Wei X, Longest PW, Venitz J, Byron PR. In Vitro Tests for aerosol deposition. IV: simulating variations in human breath profiles for realistic DPI testing. *J Aerosol Med Pulm Drug Deliv.* 2016;29(2):196–206. <https://doi.org/10.1089/jamp.2015.1215>.
- Zhou Y, Sun J, Cheng Y-S. Comparison of deposition in the USP and physical mouth–throat models with solid and liquid particles. *J Aerosol Med Pulm Drug Deliv.* 2011;24(6):277–84. <https://doi.org/10.1089/jamp.2011.0882>.
- Javaheri E, Shemirani FM, Pichelin M, Katz IM, Caillibotte G, Vehring R, et al. Deposition modeling of hygroscopic saline aerosols in the human respiratory tract: comparison between air and helium–oxygen as carrier gases. *J Aerosol Sci.* 2013;64:81–93. <https://doi.org/10.1016/j.jaerosci.2013.04.010>.
- Chan TL, Lippmann M. Experimental measurements and empirical modeling of the regional deposition of inhaled particles in humans. *Am Ind Hyg Assoc J.* 1980;41(6):399–409. <https://doi.org/10.1080/15298668091424942>.
- Heyder J. Gravitational deposition of aerosol particles within a system of randomly oriented tubes. *J Aerosol Sci.* 1975;6(2):133–7. [https://doi.org/10.1016/0021-8502\(75\)90006-3](https://doi.org/10.1016/0021-8502(75)90006-3).
- Heyder J, Gebhart J. Gravitational deposition of particles from laminar aerosol flow through inclined circular tubes. *J Aerosol*

- Sci. 1977;8(4):289–95. [https://doi.org/10.1016/0021-8502\(77\)90048-9](https://doi.org/10.1016/0021-8502(77)90048-9).
29. Ingham DB. Diffusion of aerosols from a stream flowing through a cylindrical tube. *J Aerosol Sci.* 1975;6(2):125–32. [https://doi.org/10.1016/0021-8502\(75\)90005-1](https://doi.org/10.1016/0021-8502(75)90005-1).
30. Finlay WH, Lange CF, King M, Speert DP. Lung delivery of aerosolized dextran. *Am J Respir Crit Care Med.* 2000;161(1):91–7. <https://doi.org/10.1164/ajrccm.161.1.9812094>.
31. Finlay WH, Stapleton KW, Chan HK, Zuberbuhler P, Gonda I. Regional deposition of inhaled hygroscopic aerosols: in vivo SPECT compared with mathematical modeling. *J Appl Physiol.* 1996;81(1):374–83. <https://doi.org/10.1152/jappl.1996.81.1.374>.
32. Finlay WH, Lange CF, Li W-I, Hoskinson M. Validating deposition models in disease: what is needed? *J Aerosol Med.* 2000;13(4):381–5. <https://doi.org/10.1089/jam.2000.13.381>.
33. Newman SP, Chan HK. In vitro-in vivo correlations (IVIVCs) of deposition for drugs given by oral inhalation. *Adv Drug Deliv Rev.* 2020;167:135–47. <https://doi.org/10.1016/j.addr.2020.06.023>.
34. Stahlhofen W, Gebhart J, Heyder J, Philipson K, Camner P. Intercomparison of regional deposition of aerosol particles in the human respiratory tract and their long-term elimination. *Exp Lung Res.* 1981;2(2):131–9. <https://doi.org/10.3109/01902148109052309>.
35. Martin AR, Finlay WH. Model calculations of regional deposition and disposition for single doses of inhaled liposomal and dry powder ciprofloxacin. *J Aerosol Med Pulm Drug Deliv.* 2018;31(1):49–60. <https://doi.org/10.1089/jamp.2017.1377>.
36. Hill LS, Slater AL. A comparison of the performance of two modern multidose dry powder asthma inhalers. *Respir Med.* 1998;92(1):105–10. [https://doi.org/10.1016/S0954-6111\(98\)90040-3](https://doi.org/10.1016/S0954-6111(98)90040-3).
37. Hindle M, Byron PR. Dose emissions from marketed dry powder inhalers. *Int J Pharm.* 1995;116(2):169–77. [https://doi.org/10.1016/0378-5173\(94\)00287-F](https://doi.org/10.1016/0378-5173(94)00287-F).
38. Hira D, Okuda T, Mizutani A, Tomida N, Okamoto H. In vitro evaluation of optimal inhalation flow patterns for commercial dry powder inhalers and pressurized metered dose inhalers with human inhalation flow pattern simulator. *J Pharm Sci.* 2018;107(6):1731–5. <https://doi.org/10.1016/j.xphs.2018.02.002>.

Publisher's Note Springer Nature remains neutral with regard to jurisdictional claims in published maps and institutional affiliations.